Journal of Archaeological Science: Reports 66 (2025) 105289

Contents lists available at ScienceDirect

Journal of Archaeological Science: Reports

journal homepage: www.elsevier.com/locate/jasrep

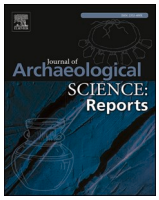

Mössbauer spectroscopy for dolerite provenance characterization in Valencia region: A proof of concept

J. Jiménez-Puerto [a,*], E. Devlin [b,*], G. Gallello [a,c], T. Orozco-Köhler [a], J. Bernabeu Aubán [a]

[a] Department of Prehistory, Archaeology and Ancient History, University of Valencia, Spain
[b] NCSR Demokritos, Athens, Greece
[c] Material Science Institute (ICMUV). University of Valencia, Spain

ARTICLE INFO

Keywords:
Mössbauer spectroscopy
Ophitic rock raw material
Neolithic

ABSTRACT

The determination of the ophitic rock provenance is of key importance for understanding the trade networks, mobility patterns, and resource exploitation strategies of Neolithic communities, as these rocks were extensively used to produce polished tools such as axes and adzes. Their role in agricultural practices and woodland management highlights their significance in the socioeconomic and cultural transformations that characterized the Neolithic period in the Mediterranean area of the Iberian Peninsula. By tracing the origins and circulation of these materials, we can gain valuable insights into the interactions, technological choices, and adaptive strategies of early agrarian societies. This study evaluates the use of Mössbauer Spectroscopy (MoS) to distinguish rocks collected from different outcrops. MoS is a powerful technique which provides detailed information on the crystal structure, magnetic state, valence state and phase composition. In this study Fe^{57} MoS which detects the iron containing phases was used. In the ophitic samples a range of iron phases were identified including magnetite, maghemite, hematite. The phase composition of samples taken from several different outcrops were compared showing differences. This may allow the use of MoS, in combination with other techniques such as XRF, petrography, as a tool in the determination of ophitic artifact provenance.

1. Introduction

Ophitic rocks were widely used during the Neolithic era for the manufacture of tools, particularly polished axes and adzes. These tools played a crucial role in agricultural and woodland management practices, which were essential during the transition to a sedentary lifestyle. In the Iberian Peninsula, the Neolithic period (approximately 5600–2500 BCE) marked significant cultural and economic transformations, including the adoption of agriculture, animal domestication, and complex social structures (Bernabeu Aubán et al., 2002; Bernabeu and Balaguer 2006; Molina & Orozco, 2011). Ophitic rocks, due to their abundant availability, durability and ability to hold a sharp edge, became a preferred raw material for tool production, often sourced from specific geological formations. Understanding the provenance of these rocks provides insights into trade networks, mobility patterns, and resource exploitation strategies of Neolithic communities in the Mediterranean region of the Iberia peninsula (Bernabeu and Balaguer 2006; Garrido-Pena, 1996; Jiménez-Puerto, 2022; Orozco-Köhler, 1990). The first studies (Orozco-Köhler, 2000; Ricq-de Bouard, 1996) focused in this area employed petrographic analysis, geochemical characterization, and spatial distribution to trace the origins and circulation of ophitic tools, shedding light on the broader socioeconomic dynamics of Neolithic societies in the region. The findings contributed to our understanding of material culture and its role in shaping early agrarian communities (Orozco-Köhler, 2000; Ricq-de Bouard, 1996).

Recently, invasive and non-invasive methodological approaches were developed in this type of materials in important archaeological sites worldwide like Stonehenge (Clarke et al., 2024). Pushing forward in this direction our research group members employing inductively coupled plasma mass spectrometry (ICP-MS) portable X-ray fluorescence (pXRF), Raman spectroscopy, and neural networks showed the potential of combining analytical techniques to differentiate geological sources of ophitic rocks and archaeological artifacts (Gallello et al., 2016; Jiménez-Puerto et al., 2024; Orozco Köhler and Gallello 2017; Ramacciotti et al., 2022). These approaches have provided valuable insights into the geochemical and mineralogical variability of ophitic materials, laying the groundwork for further development of provenance analysis methodologies.

While techniques such as portable X-ray fluorescence (pXRF) and inductively coupled plasma mass spectrometry (ICP-MS) provide

* Corresponding authors.

https://doi.org/10.1016/j.jasrep.2025.105289
Received 20 March 2025; Received in revised form 28 May 2025; Accepted 23 June 2025

valuable elemental composition data, they may face some limitations for ophitic rock provenance studies. For example, these methods cannot distinguish between different mineral phases containing the same elements, and especially for pXRF, surface effects often compromise the detection of critical elements like Fe and Al (Ogburn et al., 2013; Potts et al., 2006; Williams-Thorpe et al., 1999). These studies have highlighted that while certain lighter elements like Al and Fe present analytical challenges due to surface effects, other elements such as Nb, Bi, and Sb have the potential to serve as reliable discriminators for source attribution.

Additionally, petrographic analysis, though informative, is often subjective and difficult to quantify. Mössbauer Spectroscopy (MoS) addresses these limitations by specifically characterizing iron-bearing mineral phases and their relative proportions – crucial discriminators in basic igneous rocks that often share similar bulk chemistry. MoS can detect subtle differences in oxidation states, magnetic properties, and crystalline environments of iron, providing a unique fingerprint that remains undetectable through elemental analysis alone. Furthermore, MoS can identify both crystalline and amorphous phases, making it particularly valuable for materials that have undergone various degrees of alteration, a common challenge in archaeological provenance studies (Murad, 1998; Murad & Cashion, 2004; Stevens & Zhu, 1986). Despite these advantages, in contrast to XRF, MoS suffers from a disadvantage i.e the minimally destructive nature of the measurement. Small pieces of the sample (total mass of the order of 250 mg) must be powdered to carry out the transmission geometry MoS used in this study.

In this study, a methodological approach was tested aiming to assess the potential applications of MoS as a complementary analytical method. The MoS group at NCSR Demokritos (Athens, Greece) was one of the first groups to apply this technique to the study of archaeology (Gangas et al., 1971; Kostikas et al., 1974; Papamarinopoulos et al., 1987). Previous works using portable X-ray fluorescence (pXRF) and neural network (Jiménez-Puerto et al., 2024) analysis have demonstrated the potential of combining advanced analytical techniques for provenance studies of ophitic materials. The application of self-organizing maps (SOM)(Kohonen, 1982) to pXRF data has shown promising results in distinguishing between different source outcrops based on their elemental compositions. Building upon these advances in non-destructive analytical approaches, this study explores the potential of MoS as a complementary technique for provenance determination.

Mössbauer Spectroscopy (MoS) can provide detailed information on the phase composition, valence states, and magnetic properties of iron-bearing minerals, which are often key discriminators in geological materials. By identifying and characterizing phases such as magnetite, hematite, maghemite, and ilmenite, MoS is a powerful tool to investigate the mineralogical variability among potential source outcrops. Furthermore, its high sensitivity to subtle changes in iron-bearing phases makes it particularly suited to provenance studies of ophitic materials, where other techniques might face limitations due to sample heterogeneity or post-depositional alterations (Stevens & Zhu, 1986).

To test the viability of MoS for this purpose, we adopt a “proof of concept” approach, focusing on a limited dataset of six geological samples from distinct ophitic outcrops in the Iberian Peninsula. These samples represent a range of geological settings and mineralogical compositions, providing a suitable framework to evaluate the discriminatory power of MoS. By comparing the Mössbauer spectra of these samples, we aim to assess whether the technique can effectively differentiate between sources based on their phase composition.

The findings of this study, at this stage focused in raw material sampled from different outcrops located in Valencia region, will serve as a critical first step toward integrating MoS into broader provenance research frameworks. If successful, this approach could be applied to archaeological artifacts, offering a complementary reliable method to trace the origins of ophitic tools. Through the integration of MoS data with elemental analysis using pXRF and multivariate statistical techniques, we aim to establish robust and reliable criteria for discriminating between different dolerite sources, contributing significantly to our understanding of prehistoric raw material procurement, mobility patterns, and trade networks in the Iberian Peninsula.

1.1. Previous applications of Mössbauer spectroscopy in archaeological studies

MoS has evolved as a significant analytical tool in archaeological research since its first applications in the late 1960s. With the appropriate source (^{57}Co) the technique’s sensitivity to specifically iron-bearing phases has made it especially valuable in archaeometry studies where iron compounds play a key role. Over the decades, its applications have expanded across various domains of archaeological research, demonstrating significant potential for material characterization and provenance studies.

The technique was initially applied primarily to ceramic studies, where it proved particularly effective in determining firing conditions and temperatures through the analysis of iron oxidation states and phase compositions (Wagner & Kyek, 2004; Wagner & Wagner, 2004; Wagner et al., 2000). These early studies established fundamental methodological approaches that would later be applied to other archaeological materials. The ability to identify specific iron phases and their magnetic properties has provided crucial information about ancient production technologies and raw material sources.

In the field of metallurgical studies, MoS has been instrumental in understanding ancient iron production techniques and corrosion processes. Studies of historical iron artifacts have revealed detailed information about manufacturing processes and conservation states (Dillmann et al., 2002), while analyses of slag materials have provided insights into early metallurgical technologies. The technique’s capacity to distinguish between different iron oxides and hydroxides has proven particularly valuable in conservation studies.

For lithic materials, which are particularly relevant to our study, MoS has demonstrated significant potential in provenance studies. The technique’s ability to identify specific mineral phases and their relative proportions has proven useful in discriminating between different geological sources (F. Wagner & Kyek, 2004). Particularly significant has been its application to basaltic rocks, where the identification of specific iron-bearing mineral assemblages has enabled the differentiation between outcrops with similar bulk compositions (Lyubutin et al., 2009). The technique can provide information about both crystalline and amorphous phases, making it especially useful for studying materials that have undergone various degrees of alteration (Murad, 1998).

One of the most significant developments in recent years has been the integration of Mössbauer spectroscopy with other analytical techniques. This complementary approach has proven particularly effective in provenance studies, where multiple lines of evidence are often necessary to establish reliable source attributions. For example, the combination of Mössbauer spectroscopy with X-ray fluorescence and petrographic analysis has enabled more robust characterization of stone tool sources (Přichystal, 2013).

Recent methodological advances have also expanded the technique’s applications. The development of improved data analysis protocols has enhanced our ability to resolve complex spectra and identify subtle differences in mineral assemblages. These advances have been particularly important for provenance studies, where the ability to detect minor variations in iron phase compositions can be crucial for discriminating between similar source materials (Schaaf, 2005).

Looking specifically at applications in the Mediterranean region, several studies have demonstrated the utility of MoS for characterizing archaeological materials. Work on Iberian ceramics and metallurgical remains has shown how the technique can provide insights into ancient production technologies and trade networks (Molera et al., 1997). MoS has also been applied to the question of obsidian artifact provenance in the western Mediterranean (G. Longworth and S.E. Warren 1979). These regional applications provide important methodological precedents for

our current study of dolerite provenance.

1.2. Geological background

The Mössbauer spectroscopy results, that will be presented later, will explore the potential of this technique for establishing distinctive signatures of dolerite sources through their iron-bearing phases. To validate this methodological approach and understand its implications for prehistoric procurement studies, it is essential to examine the geological context and specific characteristics of the analyzed outcrops. This detailed examination of the regional distribution and geological setting of the dolerite sources provides the framework necessary to assess the reliability and applicability of MoS for provenance determination.

Recent analytical studies utilizing portable XRF have mapped the geochemical variability across these outcrops, providing baseline data on elemental distributions. These analyses have shown that despite the challenges of surface weathering and alteration, distinct geochemical signatures can be identified for different source locations. The present MoS study aims to complement these existing datasets by providing detailed information about iron-bearing phases, which may offer additional discriminating parameters for provenance determination. The combination of multiple analytical approaches – including petrographic analysis, XRF elemental mapping, and MoS – creates a more robust framework for understanding the geological and mineralogical variability of these important raw material sources.

The Valencia region is characterized predominantly by sedimentary lithologies, with scarce outcrops of metamorphic, volcanic, and subvolcanic materials. The dolerite outcrops studied here (see Fig. 1) are typically associated with deep tectonic structures, with their surface presence usually linked to Keuper (Upper Triassic) formations (Orozco-Köhler 2000).

The studied outcrops present a distinctive distribution across the region. Santa Eulalia-Villena is situated in the northern area. The Barxeta outcrop is located between the towns of Barxeta and Lloc Nou de Fenollet, and has been exploited as an aggregate quarry. The material exhibits textural variations from slightly trachytic to subophitic-diabasic, sharing similarities with the Cerro Negro materials from Quesa.

The Pinós outcrop is located on the eastern slope of Cabezo de la Sal. This outcrop, along with others in the area (Xinorlet-Font d'Almorquí and Sax), follows a structural tectonic alignment determined by the intersection of various faults.

The Náquera outcrop, situated southeast of Náquera town, represents a small volume of basic igneous rocks. The materials are classified as dolerites with andesine and labradorite, showing significant alteration.

The Quesa outcrop, specifically located at Cerro Negro in the Canal de Navarrés near the Escalona River basin, represents an intensively exploited ancient quarry. This outcrop shows considerable grain size variation and structural variability in its diabase with labradorite composition.

A significant geological pattern emerges when comparing these outcrops: materials within the Iberian domain show considerably more alteration than those located in the Betic domain, reflecting different orogenic conditions that have affected these territories. Most of these outcrops have been intensively exploited as modern quarries, primarily for aggregate production, which has significantly altered their original appearance and, in some cases, led to near-complete depletion. This recent exploitation activity poses challenges for archaeological studies, as it has modified or destroyed evidence of prehistoric exploitation.

The identification of these sources as potential raw material procurement sites for prehistoric communities is based not only on their geological characteristics but also on their accessibility and the quality of the raw material they provide (Carrión & Gómez, 1983). The varying degrees of preservation and alteration across different outcrops suggest that prehistoric communities (Fig. 1) would have had access to materials of varying quality, which may have influenced their procurement strategies and tool production techniques (Orozco-Köhler, 2000).

2. Materials and methods

As described in the previous sections, the dolerite outcrops in the Valencia region present distinct mineralogical and petrographic characteristics that may serve as indicators for provenance studies. To test the potential of Mössbauer spectroscopy for establishing reliable source discrimination, a systematic sampling strategy was implemented across

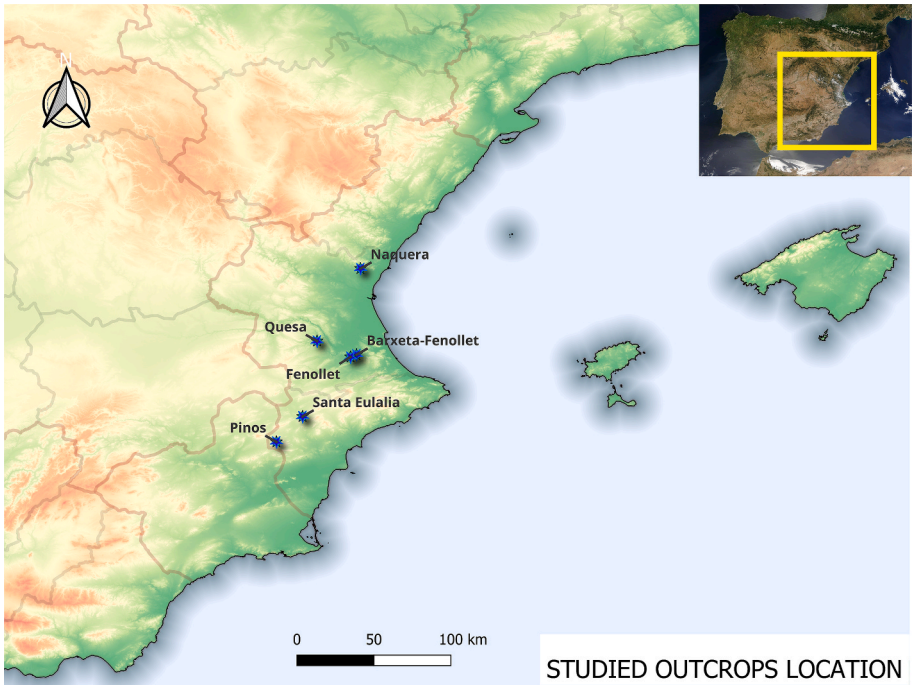

Fig. 1. Sampled outcrops involved in the study and potential settlements that may employed lithic raw materials in the region.

the main outcrops. Previous research has demonstrated the importance of systematic sampling strategies in provenance studies, particularly when dealing with weathered archaeological materials (Polikreti et al., 2011; Schwedt et al., 2004).

Rock samples were collected from six major dolerite outcrops in the Valencia region: Santa Eulalia-Villena in the northern area, Barxeta-Fenollet situated between the towns of Barxeta and Lloc Nou de Fenollet, Pinós located on the eastern slope of Cabezo de la Sal, Náquera situated southeast of Náquera town, Fenollet, and Quesa located at Cerro Negro in the Canal de Navarrés (Fig. 1). Fresh samples (5–10 g) were collected from each outcrop, selecting material with minimal weathering to ensure the reliability of the analyses. The coordinates of all sampling points were included in the supplementary material in CSV format. The sampling strategy at each outcrop followed a systematic protocol, selecting multiple points (3–5) per outcrop separated by at least 5–10 m when the dimensions of the outcrop allowed to capture possible lateral variability.

The sampling strategy was designed considering outcrop accessibility, geological homogeneity within individual dolerite intrusions, and the proof-of-concept nature of this study. While statistical guidelines recommend larger sample sizes (Aldenderfer & Drennan, 1998), our systematic approach prioritized geological representativeness, collecting fresh samples from multiple points per outcrop to capture lateral variability while providing sufficient material for both analytical techniques.

Mössbauer spectroscopy was carried out with a ^{57}Co(Rh) source in constant acceleration mode at room temperature. The spectrometer was calibrated using a thin iron foil. Powder samples were prepared by hand grinding in an agate mortar. All the spectra were obtained at room temperature. Fitting was carried out using the IMSG program (Douvalis et al., 2010).

2.1. Comparative analysis

This study employs a strategic combination of Mössbauer Spectroscopy (MoS) and portable X-ray Fluorescence (pXRF) to overcome the limitations inherent in individual analytical techniques when applied to dolerite provenance studies. Table 1 summarizes the comparative advantages and limitations of the main techniques commonly used in lithic provenance research.

The Mössbauer Spectroscopy approach employed in this study shares fundamental principles with other spectroscopic methods for detecting iron oxides and minerals. While Mössbauer identifies iron phases through nuclear resonance absorption, other techniques such as reflectance spectroscopy detect characteristic absorption features through electronic transitions and crystal field effects. For instance, Fe^{2+} in ferrous oxide typically exhibits broad NIR absorption features around 1 μm and sometimes at 2 μm in reflectance spectra, resulting from crystal field splitting and Fe-O lattice vibrations. Similarly, our Mössbauer spectra reveal distinct hyperfine parameters (isomer shift, quadrupole splitting, and hyperfine field) that uniquely characterize iron species including magnetite, hematite, and maghemite. This complementarity suggests potential for a future integrated approach combining minimally destructive Mössbauer analysis with non-destructive reflectance or Raman spectroscopy. Such integration would be particularly valuable for archaeological artifacts where limited sampling is preferable, allowing non-destructive techniques to be calibrated against the more definitive phase identifications provided by Mössbauer Spectroscopy, as mentioned in our discussion of future research directions.

The integrated approach developed in this study leverages the complementary strengths of MoS and pXRF while mitigating their individual limitations. Specifically, pXRF provides rapid, multi-element characterization that establishes the bulk geochemical signature, while MoS delivers detailed information about iron speciation that is unattainable through elemental analysis alone. This combination is particularly valuable for dolerite materials where iron phases often serve as key discriminators despite similar bulk chemistry.

The theoretical detection limit for iron phases using MoS is approximately 2–3 % of the total iron content when optimal sample preparation and acquisition parameters are employed (Dyar et al., 2006; Murad, 1998). For pXRF, detection limits for iron typically range from 50-100 ppm for total elemental content being in the studied material higher than percentage (Gallello et al. 2016), but the technique cannot distinguish between different mineral phases containing the same element. By combining these techniques, we aim to capture both bulk compositional variations (through pXRF) and mineralogical differences in iron speciation (through MoS) that may reflect different geological origins or formation processes.

Table 1
Comparative analysis of analytical techniques for dolerite provenance studies.

Technique	Parameters Measured	Advantages	Limitations	Detection Limits for Fe	Sample Preparation
Mössbauer Spectroscopy (Dyar et al., 2006; Klingelhöfer et al., 2004)	Fe oxidation states, coordination environment, magnetic properties, mineral phases	Distinguishes between Fe-bearing phases; sensitive to mineral structure; detects both crystalline and amorphous phases	Limited to Fe-bearing minerals; requires reference spectra for identification	0.1–0.5 wt% Fe in bulk sample; can detect mineral phases at 2–3 % of total Fe content	Minimally destructive; powder sample (50–100 mg)
pXRF (Frahm & Doonan, 2013; Potts & West, 2008)	Elemental concentrations (major, minor, trace elements)	Non-destructive; rapid; portable; multi-element capability	Surface effects; matrix effects; limited to elements > Mg; lower precision than lab-based techniques	50–100 ppm for total Fe; cannot distinguish mineral phases	Non-destructive; minimal or no preparation
ICP-MS (Ammann, 2007; Thomas, 2013)	Elemental concentrations with isotopic discrimination	High sensitivity; low detection limits; excellent precision; full elemental range	Destructive; complex sample preparation; no mineral phase information; high cost	1–5 ppb for total Fe; cannot distinguish mineral phases	Minimally destructive (15–50 mg); acid digestion required
LA-ICP-MS (Liu et al., 2008; Sylvester & Jackson, 2016)	Elemental concentrations with isotopic discrimination	Good sensitivity; low detection limits; excellent precision; full elemental range	Micro-destructive; no mineral phase information; high cost	1–5 ppb for total Fe; cannot distinguish mineral phases	Minimal or no preparation
Petrography (Higgins, 2006; Vernon, 2018)	Mineral identification, textural relationships, alteration patterns	Direct observation of mineral assemblages and textures; contextual information	Subjective; difficult to quantify; requires expertise; destructive	Qualitative only	Destructive; thin section preparation
FTIR/Raman (Froment et al., 2008; Smith & Clark, 2004)	Mineral phase identification, molecular bonds	Non-destructive; minimal sample preparation; sensitive to both crystalline and amorphous phases	Surface analysis only; fluorescence interference; limited quantification	Qualitative only for Fe phases	Minimal or no preparation

2.2. The samples

The sampling strategy for this proof-of-concept study was designed to test the potential of MoS for discriminating between different dolerite sources in the Valencia region. Our approach combines detailed geological and petrographic information to provide a robust contextual framework for the interpretation of the Mössbauer data. The selection of sampling locations was based on previous archaeological studies that have identified these outcrops as potential sources for Neolithic polished stone tools (Orozco-Köhler 2000), as well as on geological surveys that have documented their distinctive characteristics. These outcrops present varying degrees of preservation and accessibility, ranging from well-preserved natural exposures to heavily exploited quarry sites, which add complexity to their characterization but also provides an opportunity to test the technique under different conditions.

The characterization of the samples follows a multi-scale approach, from the regional geological context to the microscopic mineral composition. The following sections present first the geological setting and distribution of the sampled outcrops, establishing their structural and stratigraphic relationships within the regional geological framework. This is followed by their detailed petrographic and mineralogical characterization, carried out by thin section observed by polarized light microscopy, which provides critical information about mineral assemblages, textures, and alteration patterns. This comprehensive characterization is essential for understanding how the iron-bearing phases identified through MoS relate to the broader geological and mineralogical context of each source, and ultimately, for evaluating the potential of this technique for archaeological provenance studies.

The samples measured are listed in Table 1. They come from the Sta Eulalia-Villena, Pinós, Fenollet, Náquera, Quesa and Barxeta (STA_EU, PIN, FEN, NAQ, QUE and BARX respectively) outcrops found in the Valencia region. For the Barxeta, Náquera and Fenollet samples, two different samples from each outcrop were prepared to examine sample reproducibility.

Textural and mineralogical characteristics

The petrographic and mineralogical characterization of dolerite outcrops across the Valencia region offers a detailed understanding of their distinct textures and mineral assemblages (Le Maitre et al., 2005). Dolerite, along with basalt and gabbro, represents a group of basic igneous rocks derived from mantle melting, with compositions largely governed by their silica content (SiO_2). These rocks are primarily distinguished by textural differences, influenced by the cooling depth during crystallization. Basalt is a fine-grained volcanic rock, typically consisting of calcic plagioclase and pyroxene, sometimes accompanied by olivine or interstitial quartz. Dolerite, on the other hand, is coarser-grained, intermediate between basalt and gabbro, often exhibiting ophitic textures and comprising plagioclase, pyroxene, and opaque minerals. Gabbro, being coarsest of the three, is an intrusive rock characterized by calcic plagioclase, pyroxene, and iron oxides. Collectively referred to as “ofitas” in Spanish literature due to their distinctive field textures, these rocks share common mineralogical features but differ texturally due to varying cooling histories.

Building upon these classifications, the present study identifies unique petrographic features of dolerite outcrops in the Valencia region, establishing a foundation for provenance analysis. The following section outlines the materials and methods, including a systematic sampling strategy aimed at testing their potential for source discrimination.

The Santa Eulalia-Villena samples are typified by a mineralogical composition dominated by plagioclase (Pl) and pyroxene (Px), with the latter undergoing transformation to amphibole (Anf), exhibiting green to brown pleochroism indicative of hornblende (Hbl) compositions. Chlorite (Chl), likely formed from altered olivine (Ol), appears as pseudomorphs, while plagioclase shows sericitic alteration. Abundant ilmenite (Ilm) is present as an opaque mineral, with some plagioclase crystals retaining polysynthetic twinning.

The Barxeta-Fenollet outcrop displays significant grain size variation, where plagioclase is extensively sericitized, and no fresh pyroxene remains, although plagioclase is more volumetrically dominant. Secondary calcite (Cc) and quartz (Qz) are present, along with accessory minerals such as ilmenite and titanite (Ttn). The material features both coarse-grained and fine-grained areas, with plagioclase forming prominent phenocrysts. Green amphibole is also observed.

The Pinós samples are characterized as volcanic rocks with very fine grain sizes, interspersed with medium-sized plagioclase phenocrysts that are heavily altered. Pyroxenes transition to amphibole and chlorite, occasionally forming radial aggregates. The matrix contains abundant ilmenite along with microcrystals of pyroxene, amphibole, and plagioclase.

Náquera outcrop material consists of fine- to medium-grained dolerite with extensive alteration. Plagioclase appears significantly degraded, described as “dirty,” with no observable fresh minerals. Chlorite and ilmenite are abundant.

The Fenollet samples closely resemble the Barxeta materials, exhibiting variable grain sizes and similar mineralogical compositions and alteration features. Plagioclase is sericitized, and pyroxenes are absent in fresh form, replaced by secondary amphibole. Calcite and quartz are also noted as secondary phases.

Quesa outcrop materials display a fine to medium grain size, with patches varying from fine to very fine. These samples show notable weathering or hydrothermal alteration. Plagioclase is transformed into sericite, while pyroxene, although preserved, exhibits alteration at the margins to amphibole.

As this work is a ’proof of concept’ specifically focused on evaluating the discriminatory potential of Mössbauer spectroscopy for provenance studies. The mineralogical descriptions were presented as geological context for interpreting the Mössbauer results, not as the main focus of the study. In future work, we plan to incorporate more detailed mineralogical characterizations through quantitative petrographic analysis.

These petrographic observations provide a detailed framework of textural and mineralogical characteristics across the dolerite outcrops, ranging from fine-grained basaltic to medium-grained doleritic textures. The distinct mineral assemblages and alteration patterns identified at each location are critical for understanding the geological processes that shaped these materials and their potential relevance in provenance studies. Building upon this foundational analysis, the subsequent section outlines the materials and methods employed, including the systematic sampling strategy and the application of Mössbauer spectroscopy, to explore the feasibility of precise source discrimination for these outcrops.

2.3. Mössbauer spectroscopy

Mössbauer spectra were collected using a conventional transmission spectrometer with a ^{57}Co(Rh) source moving with constant acceleration at RT calibrated with a thin ion foil. Isomer shifts are given with respect to metallic iron at RT. Mössbauer spectra were least-squares fitted using the IMSG program [Douvalis, A.P., Polymeros, A., Bakas, T.: IMSG-09: A ^{57}Fe–^{119}Sn Mössbauer spectra computer fitting program with novel interactive user interface. J. Phys. Conf. Ser. 217, 012014(4 pp) (2010)]. The samples were prepared by selecting un-weathered pieces from the collected samples which were then ground by hand to a fine powder in an agate mortar and pestle.

Mössbauer spectroscopy presents inherent challenges for establishing conventional precision and accuracy values. The hyperfine parameters derived from fitting algorithms typically underestimate the actual uncertainty due to factors such as spectral component overlap, texture effects, and thickness variations. We have applied conservative error values to avoid unrealistic claims about analytical precision, considering that these estimates do not affect the study’s conclusions regarding significant differences between outcrops. The reproducibility demonstrated in duplicate samples from Barxeta, Náquera, and Fenollet

provides additional evidence of the method's reliability.

2.4. Portable X-ray fluorescence analysis (PXRF)

Elemental analyses were performed using a portable X-ray fluorescence spectrometer. The pXRF device employed is a Vanta CSeries Handheld XRF Analyzer including rhodium (Rh) anode 40 kV X-ray tube, SDD (Silicon Drift Detector). The measurement spot is characterised by Single-click 3 mm diameter collimation. Acquisition time was 60 s and calibration GeoChem 2-beam METHOD-G2-VCR was used.

Measurements were taken directly on the sample surfaces, which were previously cleaned to remove potential surface contamination. Three measurements per sample were conducted to assess homogeneity, using an acquisition time of 60 s per measurement. The analyzed

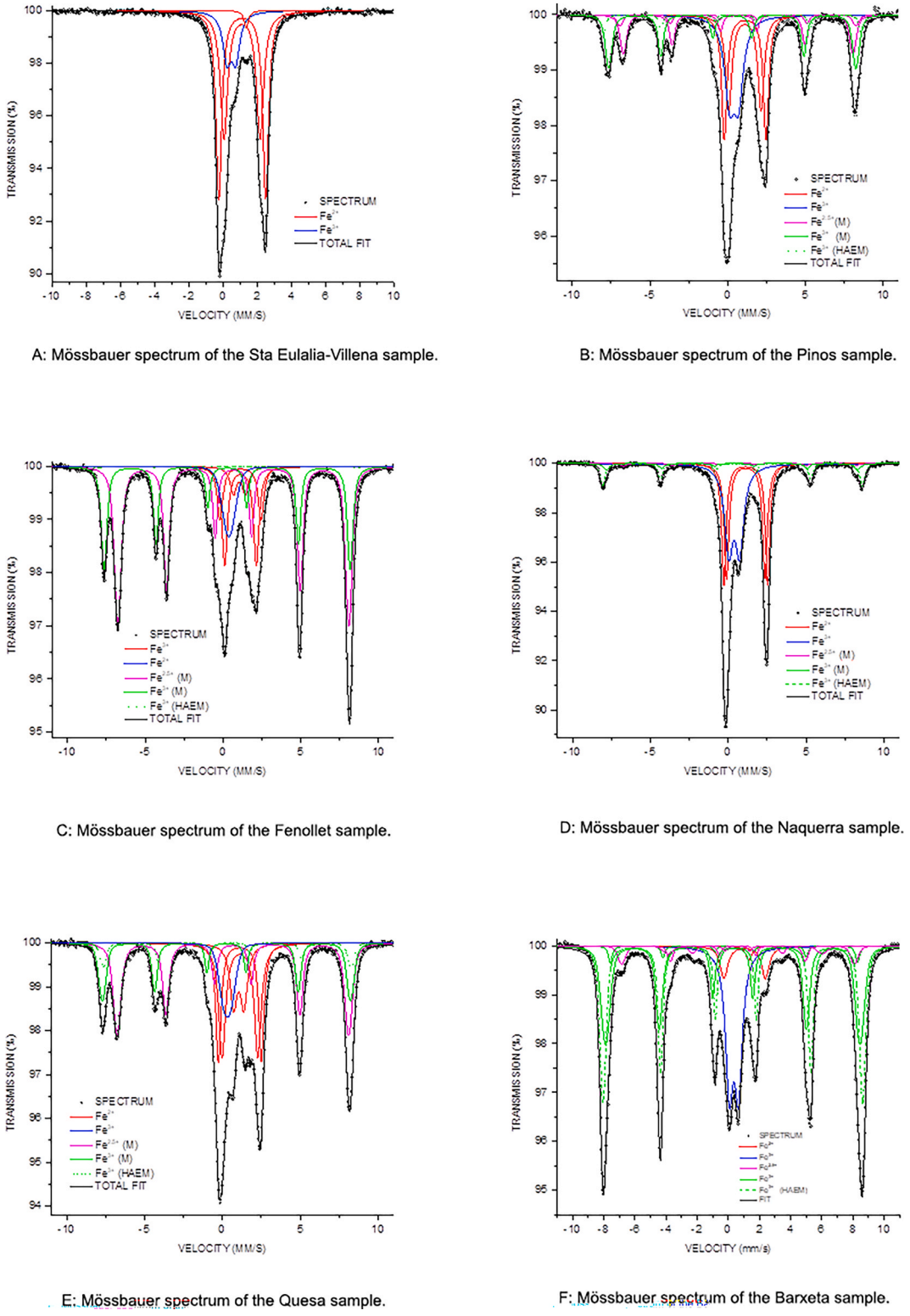

Fig. 2. Mössbauer Spectra of the six samples.

elements included major elements (Fe, Ti, Mn) and trace elements (V, Cr, Co, Ni), selected for their relevance in the characterization of mafic rocks.

2.5. Data processing

Statistical analysis and data processing were performed using Python (v3.8) (McKinney, 2010; Pedregosa et al., 2011; Van Rossum & Drake, 2014) with specialized libraries including pandas for data manipulation, scikit-learn for multivariate analysis, and scipy for statistical computations. The raw pXRF data were first processed to ensure measurement quality by converting all measurements to numeric format. Outlier detection using the interquartile range method was considered but not implemented due to the small sample size (n = 6 outcrops), which makes IQR-based outlier detection statistically unreliable. All measurements were retained to preserve the maximum information content from this proof-of-concept dataset. Principal Component Analysis (PCA) was performed on standardized (z-score) elemental data to reduce dimensionality and identify patterns in the multivariate dataset. The PCA included seven elements (Fe, Ti, V, Cr, Mn, Ni, Co) selected based on their measurement reliability. Correlation analyses between total Fe content and Mössbauer-identified phases were conducted using Pearson's correlation coefficient. All visualizations were generated using matplotlib and seaborn libraries (Hunter, 2007; Waskom, 2021), with a focus on clear representation of multivariate relationships and phase distributions.

3. Results

The combination of Mössbauer spectroscopy data with elemental analysis and subsequent multivariate statistical treatment revealed distinctive patterns in both iron phase distribution and elemental associations across the studied outcrops, providing multiple levels of discrimination between sources.

The spectra are shown in Fig. 2A-2F below. Non-magnetic ferric iron subspectra are coloured red while non-magnetic ferrous subspectra are blue. The spectrum of the Sta Eulalia sample, Fig. 1A, stands out for the absence of any magnetic component. The other samples contain varying amounts of the magnetic oxides, magnetite, maghemite, and hematite. The magnetic spectra subcomponents are separated into trivalent iron, Fe^{3+} (M), intermediate valence iron, $Fe^{2.5+}$ (M) arising from the magnetite B-sites, and Fe^{3+} (HAEM) iron which arises from hematite. The Fe^{3+}(M) component is comprised of the ferric iron present in the A-site of magnetite and the ferric iron in maghemite. These components unfortunately overlap and cannot be distinguished. However, an estimate of the relative proportions of A-site iron magnetite and maghemite ferric iron in this Fe^{3+} (M) component can be obtained assuming stochiometric magnetite which has a 1:2 occupation ratio for the A:B sites. The analysis is described below.

Mössbauer spectroscopy using a ^{57}Co source is sensitive only to iron containing phases, so the spectra are fitted with subspectra arising from phases such as olivine and pyroxene, iron sulfide (pyrrhotite, troilite, greigite), magnetite, maghemite, and hematite. These phases are present in markedly different amounts across the samples from the various outcrops which is evident from the distinctly different spectra obtained.

Table 2
Consolidated Mössbauer Data from Sta Eulalia, Pinós, Fenollet, Náquera, Quesa, and Barxeta.

Sample	Phase	Site	IS (mm/s) (+/- 0.03)	QS (mm/s) (+/- 0.03)	HF (kOe) (+/- 3)	Percentage (%) (+/- 3)
Sta Eulalia	Olivine/Pyroxene/Silicate/Illite	Fe^{2+}	1.13	2.74		45
Sta Eulalia	Olivine/Pyroxene/Silicate/Illite	Fe^{2+}	1.12	2.11		38
Sta Eulalia	Olivine/Pyroxene/Silicate/Illite	Fe^{2+}	1.37	0.00		2
Sta Eulalia	Olivine/Pyroxene/Silicate/Illite	Fe^{3+}	0.49	0.51		15
Pinós	Olivine/Pyroxene/Silicate/Illite	Fe^{2+}	1.13	2.68		20
Pinós	Olivine/Pyroxene/Silicate/Illite	Fe^{2+}	1.11	2.08		18
Pinós	Olivine/Pyroxene/Silicate/Illite	Fe^{3+}	0.41	0.57		22
Pinós	Hematite		0.41	−0.19	515	5
Pinós	Magnetite B-Site		0.68	−0.04	472	4
Pinós	Magnetite B-Site		0.69	−0.03	459	13
Pinós	Magnetite A-Site/Maghemite		0.30	0.00	494	19
Fenollet	Olivine/Pyroxene/Silicate/Illite	Fe^{2+}	1.14	2.64		7
Fenollet	Olivine/Pyroxene/Silicate/Illite	Fe^{2+}	1.13	2.03		12
Fenollet	Olivine/Pyroxene/Silicate/Illite	Fe^{2+}	1.06	0.78		4
Fenollet	Olivine/Pyroxene/Silicate/Illite	Fe^{3+}	0.39	0.26		8
Fenollet	Hematite		0.39	−0.19	518	<1
Fenollet	Magnetite B-Site		0.68	−0.01	462	44
Fenollet	Magnetite A-Site/Maghemite		0.27	0.00	492	25
Náquera	Olivine/Pyroxene/Silicate/Illite	Fe^{2+}	1.13	2.81		26
Náquera	Olivine/Pyroxene/Silicate/Illite	Fe^{2+}	1.13	2.47		26
Náquera	Olivine/Pyroxene/Silicate/Illite	Fe^{3+}	0.38	0.69		33
Náquera	Hematite		0.38	−0.20	518	10
Náquera	Hematite		0.32	−0.15	501	4
Náquera	Magnetite B-Site		0.69	−0.03	459	1
Quesa	Olivine/Pyroxene/Silicate/Illite	Fe^{2+}	1.13	2.76		14
Quesa	Olivine/Pyroxene/Silicate/Illite	Fe^{2+}	1.13	2.29		18
Quesa	Olivine/Pyroxene/Silicate/Illite	Fe^{2+}	1.05	0.66		10
Quesa	Olivine/Pyroxene/Silicate/Illite	Fe^{3+}	0.32	0.49		9
Quesa	Hematite		0.41	−0.19	494	6
Quesa	Magnetite B-Site		0.68	0.00	462	28
Quesa	Magnetite A-Site/Maghemite		0.26	0.00	495	16
Barxeta	Olivine/Pyroxene/Silicate/Illite	Fe^{2+}	1.06	2.67		5
Barxeta	Olivine/Pyroxene/Silicate/Illite	Fe^{2+}	1.33	0.00		1
Barxeta	Olivine/Pyroxene/Silicate/Illite	Fe^{3+}	0.37	0.59		20
Barxeta	Hematite		0.39	−0.19	518	35
Barxeta	Maghemite		0.29	0.00	507	30
Barxeta	Magnetite B-Site		0.62	0.02	464	5
Barxeta	Magnetite A-Site		0.39	−0.04	493	<3
Barxeta	$Fe_{1-x}S$		0.84	0.48	308	<3

The data presented in Table 2 contains the fitted hyperfine parameters for the various subspectra of each sample spectrum which allows their assignment to phases commonly found in dolerite minerals. The subspectra associated with non-magnetic phases (Olivine, pyroxenes, plagioclase, illite, silicates etc), cannot be accurately differentiated due to their broad and overlapping character so they are simply classed into ferrous and ferric subspectra.

In our analysis, magnetic iron phases were identified based on their characteristic hyperfine parameters. Magnetite was distinguished by its two magnetic subspectra: the ferric iron A-site component (IS ≈ 0.26–0.30 mm/s, HF ≈ 490–495 kOe) and the mixed-valence B-site component (IS ≈ 0.62–0.69 mm/s, HF ≈ 459–472 kOe). Maghemite was identified by its single ferric iron sextet with hyperfine parameters similar to the A-site of magnetite but with slightly higher hyperfine field values (HF ≈ 500–507 kOe). Hematite was clearly distinguished by its characteristic sextet with IS ≈ 0.38–0.41 mm/s, negative quadrupole splitting (QS ≈ −0.19 to −0.20 mm/s), and HF ≈ 515–518 kOe. These identifications are consistent with established values reported in the literature for these iron oxide phases.

Magnetic hematite is identified by its characteristic quadrupole interaction, the B-site from magnetite by its large isomer shift, and the magnetite A-site and maghemite by their hyperfine fields, ferric isomer shift and minimal or absent quadrupole interaction. Finally, a small amount of a magnetic and non-magnetic phases which may arise from iron sulfides, attributed to non-stochiometric $Fe_{1-x}S$, marcasite or greigite, was observed in one of the samples: an exact attribution to a specific sulfide phase is not possible owing to the small amount present and its overlap with other components.

The data from Table 2 are summarized in Table 3 which shows the clear differences between the various samples. This table also includes the data from the repeated samples of the Barxeta, Náquera and Fenollet outcrops which shows the sample consistency. The values given for Magnetite content are approximated by assuming that the magnetite B-site has an equivalent A-site with stochiometric content (A:B ratio of 1:2). The maghemite content is then simply what remains of the combined maghemite/magnetite A-Site when the calculated magnetite A-site component is subtracted.

Detailed analysis of the Mössbauer spectra reveals distinct patterns in the iron phase distributions across the different outcrops. The non-magnetic components show characteristic distributions, with Santa Eulalia presenting a unique pattern consisting exclusively of non-magnetic components (85 % ferrous and 15 % ferric iron), while Náquera exhibits the second-highest proportion of non-magnetic components (84–85 % total). The remaining sites display varying but consistently lower proportions of these components.

The magnetic phases demonstrate a clear gradient across the sampling sites. The total magnetic component content ranges systematically from complete absence in Santa Eulalia (0 %) through intermediate values in Náquera (15 %), Pinós (41 %), and Quesa (50 %), to high concentrations in Fenollet (69 %) and Barxeta (74 %). The magnetite content is particularly distinctive, with Fenollet containing the highest proportion (66 %) while Barxeta and Náquera show minimal amounts (4–7 % and 1–4 % respectively).

Sample consistency is demonstrated through the duplicate analyses of the Barxeta, Náquera, and Fenollet outcrops. Barxeta samples maintain consistent proportions of hematite (34–35 %) and maghemite (28–30 %), while Fenollet samples show stable magnetite content (66 %) across both measurements. Náquera samples exhibit consistent total magnetic component proportions in the repeated analyses.

Several distinctive features emerge from the data. Barxeta is unique in containing detectable iron sulfide phases (2–3 % $Fe_{1-x}S$). Fenollet shows a characteristic combination of very high magnetite content (66 %) with low hematite (3–4 %) and maghemite (2–3 %) proportions. Quesa presents an intermediate profile with balanced magnetite (42 %) and relatively low hematite and maghemite content. These distinctive patterns in iron phase compositions provide potential fingerprints for source discrimination, particularly when considering the relative proportions of magnetic versus non-magnetic components and the specific distribution of magnetic phases.

3.1. Elemental analysis and correlation with mineral phases

The analysis of Fe phases identified by Mössbauer spectroscopy (Fig. 3) reveals distinctive patterns in the distribution of iron species across the samples. STA_EU shows an almost exclusively non-magnetic profile dominated by ferrous iron (85 %), while FEN and QUE are characterized by high magnetite content (66 % and 42 % respectively). BARX presents a unique pattern with significant proportions of all three magnetic phases: hematite (35 %), maghemite (30 %), and magnetite (7 %), suggesting a more complex alteration history.

The pXRF analysis results (supplementary material) reveal significant variations in total Fe concentrations among samples, ranging from 5.4 % to 12 %, with QUE and FEN showing the highest values (>10 %) and PIN the lowest (54 %). Principal component analysis (Fig. 4) of the analyzed elements demonstrates that two components explain 81.49 % of the total variability (PC1: 63.89 %, PC2: 17.60 %), indicating that the selected elemental suite effectively captures the main geochemical variations between outcrops.

The distribution of samples in the PCA space shows a clear separation between outcrops. PIN and QUE appear at opposite ends of PC1, suggesting fundamentally different elemental compositions, particularly in their Fe, Ti, and Co contents which show strong negative loadings on this axis. NAQ and BARX/FEN contrast strongly along PC2, which is primarily influenced by V (positive loading) and transition metals Ni/Cr (negative loadings). STA_EU occupies an intermediate position, suggesting a more balanced elemental composition. These distinct groupings in the PCA space provide a first level of discrimination between sources based on their elemental signatures.

Further exploration of PC1 versus PC3 (13.61 % explained variance) reveals additional discriminatory patterns not evident in the standard PC1-PC2 analysis (Fig. 5). This complementary perspective demonstrates a distinctive triangular distribution of samples, with NAQ

Table 3
Sample phase compositions by relative iron content. (Compositions sum above 100% from rounding errors.).

Sample	Non-magnetic iron (%) (+/- 3 %)		Magnetic iron (at%) (+/- 3 %)			
	Ferrous Iron	Ferric	Magnetite	Hematite	Maghemite	$Fe_{1-x}S$
Sta Eulalia	85	15	–	–	–	–
Barxeta	6	20	7	35	30	3
	6	21	9	34	28	2
Pinós	38	22	25	5	10	–
Náquera	52	32	4	11	<1	–
	52	33	2	13	–	–
Fenollet	23	8	66	3	2	–
	22	9	66	4	3	–
Quesa	42	9	42	6	2	–

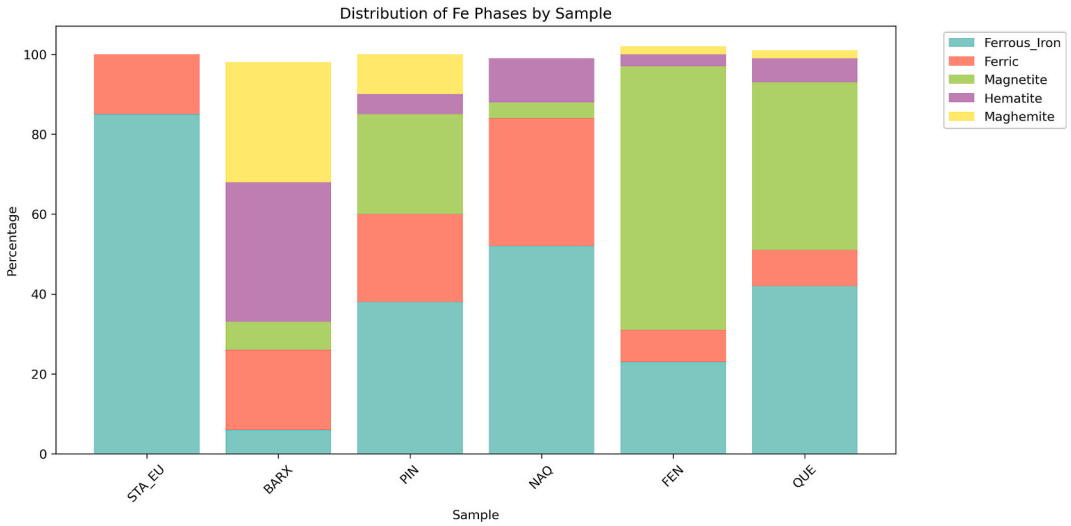

Fig. 3. Fe Phase distribution by sample.

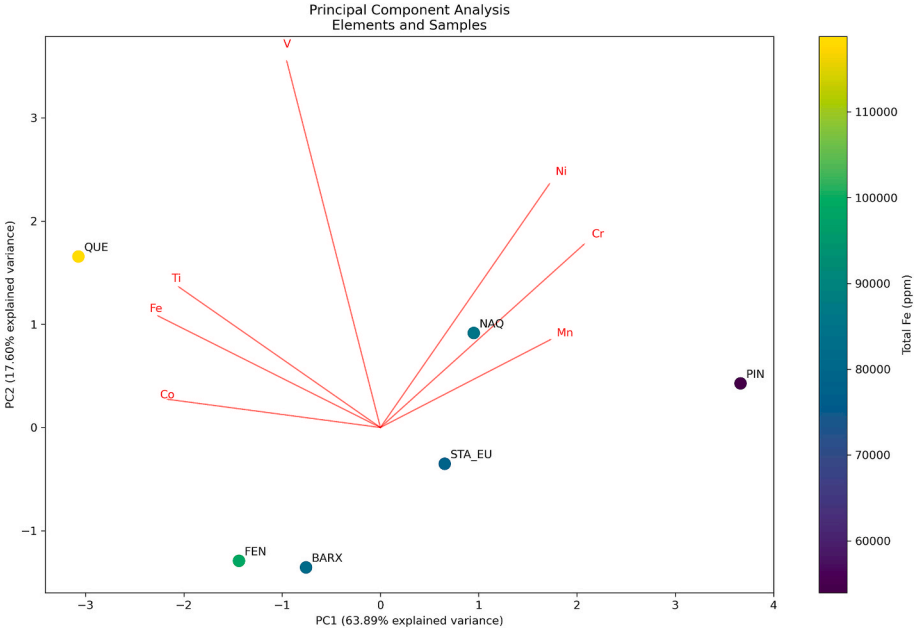

Fig. 4. PC1 vs PC2 with elements concentration measured with pXRF.

isolated in negative PC3 space (strongly associated with Ni content), PIN positioned in positive PC3 space (despite its low Fe content), and QUE maintaining its characteristic high-Fe position. Notably, Mn exhibits remarkably strong loading on PC3, suggesting its potential as a significant discriminatory element not fully captured in the principal PC1-PC2 plane. The clear opposition between Mn (positive PC3) and Ni (negative PC3) establishes an additional mineralogical dimension that further differentiates between outcrops. This supplementary analysis enhances our provenance characterization by revealing subtler geochemical signatures, particularly for samples like NAQ and PIN, which might otherwise appear less distinctive in the primary component space. The multi-dimensional discrimination observed across different principal component combinations reinforces the robust nature of elemental fingerprinting for dolerite provenance determination.

The correlation analysis between total Fe and different Fe phases (Fig. 6) provides insights into the relationship between bulk composition and mineral speciation. The moderate positive correlation with magnetite (r = 0.49) suggests that samples with higher total Fe tend to preserve more primary magnetic phases. Conversely, the significant negative correlation with ferric Fe (r = -0.56) indicates that samples with lower total Fe content have undergone more extensive oxidation, possibly due to weathering processes.

The distribution of magnetic phases relative to total Fe content is shown in Fig. 7, where each sample is represented by three points corresponding to its magnetite (blue), hematite (red), and maghemite (green) percentages. This visualization allows us to observe both total Fe variations across sources and how this iron is distributed among different magnetic phases. For example, while FEN and QUE show similar total Fe contents (around 11 %-12 %), their magnetic phase distributions differ markedly - FEN shows a dominant magnetite component (66 %), while QUE shows a more moderate magnetite content (42 %). Similarly, BARX displays a unique pattern with substantial proportions of both hematite (35 %) and maghemite (30 %), despite having intermediate total Fe content. This multi-phase representation helps identify distinctive mineralogical signatures for each outcrop that could be valuable for provenance determination.

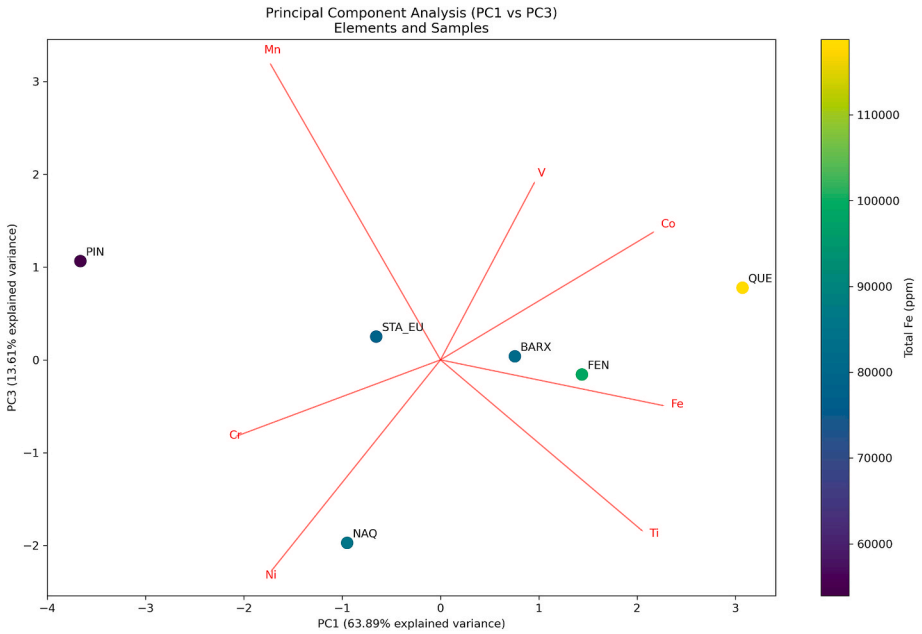

Fig. 5. PC1 vs PC3 with elements concentration measured with pXRF.

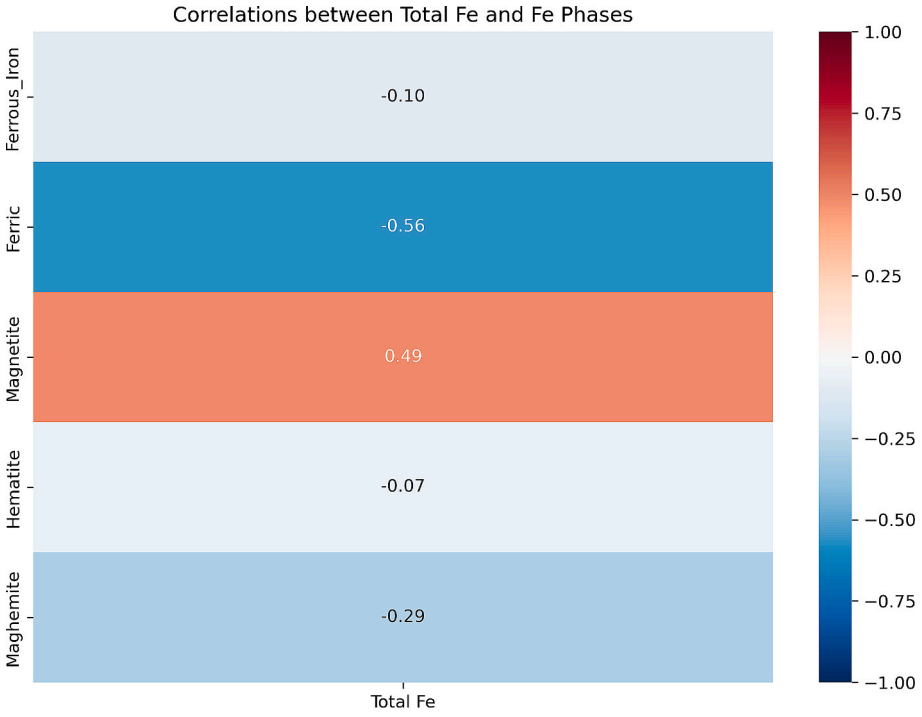

Fig. 6. Correlations between Total Fe and Fe Phases.

Within these clusters, the samples show different patterns of magnetic phase distribution. For example, while FEN and QUE have similar total Fe contents, FEN shows a much higher proportion of magnetite (66 % vs 42 %). Similarly, within the mid-Fe group, BARX shows uniquely high proportions of hematite and maghemite compared to other samples with similar total Fe content.

These results demonstrate that the combination of bulk elemental analysis and Fe phase speciation provides multiple, complementary criteria for discriminating between ophitic sources, with some outcrops showing distinctive signatures in either their elemental composition, Fe phase distribution, or both.

4. Discussion & conclusions

The results of this proof-of-concept study demonstrate that MoS can effectively differentiate between dolerite outcrops based on their iron phase compositions. The methodology reveals multiple levels of discrimination valuable for archaeological provenance studies, with several key advantages identified in our analysis.

Precision and Methodological Reliability.

The precision of MoS for quantifying iron-bearing phases has been extensively evaluated through duplicate analyses of samples from Barxeta, Náquera, and Fenollet outcrops. Results demonstrate excellent

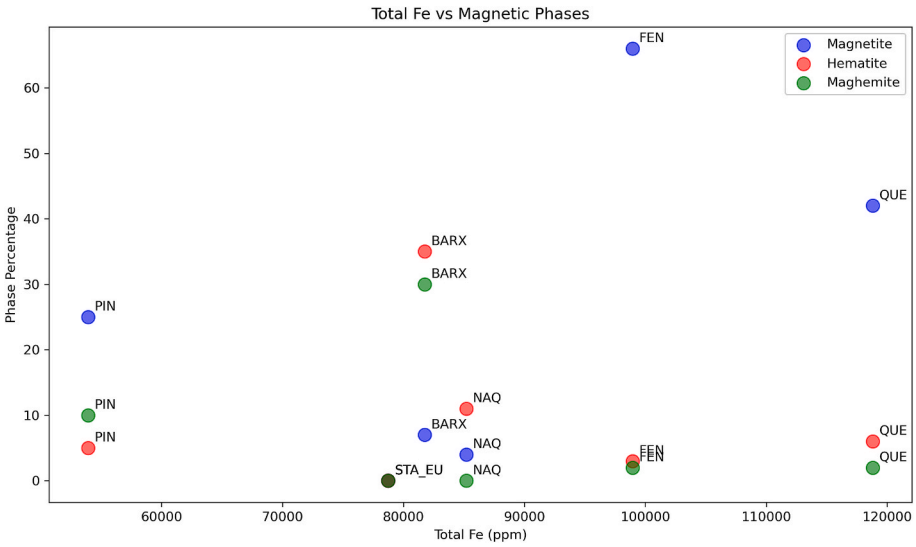

Fig. 7. Total Fe vs Magnetic Phases. The plot shows the percentage distribution of three magnetic phases (magnetite, hematite, and maghemite) against total Fe content for each sample. Each sample appears three times in the plot (once for each magnetic phase), allowing direct comparison of phase proportions across samples with different total Fe contents.

reproducibility with variations typically within ± 3 % for phase percentages, even for minor components present at levels of 2–5 %. For major iron phases (magnetite, hematite, and maghemite), MoS can reliably distinguish differences of approximately 5 % in relative abundance between samples. The detection limit for individual iron phases is approximately 2–3 % of the total iron content, allowing identification of diagnostic minor phases such as the iron sulfides detected exclusively in Barxeta samples.

Multi-level Discrimination Criteria.

Our analysis identified several hierarchical levels of discrimination between dolerite sources. The most prominent discriminator is the total magnetic component gradient observed across outcrops, which increases systematically from Santa Eulalia (0 %) through Náquera (15 %), Pinós (41 %), Quesa (50 %), and Fenollet (69 %) to Barxeta (74 %). This clear progression provides a first-order discriminator for source attribution.

Beyond total magnetic content, distinctive combinations of iron phases create characteristic fingerprints for each outcrop. Santa Eulalia's exclusively non-magnetic profile (85 % ferrous, 15 % ferric) stands out as unique, while Fenollet's combination of very high magnetite (66 %) with low hematite and maghemite content provides a distinctive signature. Even when outcrops share similar total magnetic component percentages, they can often be distinguished by their specific phase ratios, as exemplified by Fenollet and Barxeta, which despite having similar total magnetic components (69 % vs 74 %), show markedly different magnetite contents (66 % vs 4–7 %).

Complementarity with Other Analytical Techniques.

The complementary nature of MoS and pXRF analysis becomes particularly evident when examining samples with similar elemental compositions but different mineralogical histories. FEN and QUE samples show comparable total Fe contents (>10 %) but markedly different distributions of magnetic phases. This mineralogical distinction, undetectable through elemental analysis alone, provides a powerful discriminatory tool for provenance determination.

Statistical treatment of the combined datasets enhances the discriminatory power beyond what either technique could achieve independently. Principal Component Analysis of pXRF data effectively separates samples based on elemental signatures (explaining 81.49 % of variance with two components), while MoS data provides a second, independent level of discrimination based on iron phase distribution.

The multi-dimensional approach to elemental analysis, exemplified by our exploration of PC1-PC3 relationships, further enhances the discriminatory power of pXRF beyond conventional bivariate analyses. The identification of Mn and Ni as significant discriminatory elements in the third principal component reveals additional mineralogical dimensions that complement the iron-phase signatures obtained through Mössbauer spectroscopy. This relationship likely reflects differing crystallization and alteration histories among outcrops – with Mn enrichment potentially indicating specific magmatic processes in PIN samples, while Ni associations in NAQ may suggest different mineral paragenesis or parent magma compositions. Such subtle elemental discriminators, particularly transition metals not directly identified through Mössbauer analysis, provide an orthogonal layer of information that strengthens provenance determination, especially for samples with ambiguous iron-phase signatures. The triangular distribution observed in PC1-PC3 space suggests at least three distinct geochemical trajectories among the sampled outcrops, reinforcing our conclusion that integrated analytical approaches yield the most robust discrimination criteria for archaeological provenance studies.

Geological and Mineralogical Insights.

The visualization of magnetic phase distributions versus total Fe content reveals patterns that reflect different geological histories and alteration processes. The high magnetite content in FEN coupled with low hematite and maghemite percentages suggests better preservation of primary magnetic minerals, while the balanced distribution of hematite and maghemite in BARX might indicate more complex alteration processes.

The correlation patterns between total Fe and identified mineral phases suggest different weathering histories at each outcrop. The strong negative correlation between total Fe and ferric Fe (−0.56) indicates that oxidation processes have been more intense in samples with lower total Fe content, while the positive correlation with magnetite (0.49) suggests that samples with higher Fe content have better preserved their primary phases. As noted by Dyar et al. (2006), these relationships between iron species can provide critical insights into geological formation processes. The varying proportions of magnetite relative to total Fe content may reflect different cooling histories or subsequent alteration processes (Cornell & Schwertmann, 2003), information particularly valuable for understanding the formation conditions and post-depositional changes that have affected each source.

Limitations and Future Directions.

Several important considerations must be addressed before

implementing this technique in archaeological practice. This proof-of-concept study examined a limited number of samples from each outcrop, and a more comprehensive sampling program is needed to establish the full range of natural variation within each source. Additionally, the effects of weathering and post-depositional processes on iron phase compositions in archaeological artifacts require thorough investigation.

The invasive nature of the technique limits access to archaeological material. However, a consistent outcrops sampling may create the condition to use MoS as a reference method to calibrate non-invasive analytical methods such as IR or Raman to observe Fe phases, all supported by AI software to be developed.

Future research should prioritize expansion of the source database through more extensive sampling of known outcrops and investigation of potential temporal changes in source signatures through analysis of geological profiles. Development of statistical frameworks for quantitative source attribution and integration with complementary analytical techniques and advanced statistical methods, including Bayesian classification approaches that have proven successful in other archaeological contexts (Armero et al., 2020; Jiménez-Puerto et al., 2024), or machine learning could create multi-proxy provenance determination protocols. Pilot studies on well-provenanced archaeological artifacts would be essential to validate the approach under real-world conditions.

Applicability to Archaeological Artifacts.

While the minimally destructive nature of Mössbauer Spectroscopy (requiring approximately 250 mg of powdered sample) presents challenges for its direct application to valuable archaeological artifacts, several methodological strategies could enable its responsible implementation. For extensive archaeological collections, analysis could be limited to fragments or already damaged pieces, preserving the integrity of complete artifacts. Alternatively, micro-sampling protocols could be developed targeting non-diagnostic or less visible areas of artifacts, employing precision micro-drilling techniques that minimize impact on the overall morphology and informational value of the object. The creation of an extensive reference database of outcrops, as initiated in this study, could eventually allow for the reduction of the amount of archaeological material needed for reliable comparative analyses. Furthermore, this reference database could serve to calibrate non-destructive techniques such as Raman spectroscopy or FTIR to indirectly identify characteristic iron phases, using machine learning algorithms to correlate spectra obtained by non-destructive techniques with phase compositions determined by MoS. This "hybrid" approach could provide an optimal balance between artifact preservation and obtaining accurate provenance information.

Archaeological Implications.

The successful application of MoS for differentiating dolerite sources could significantly impact our understanding of prehistoric trade networks and resource exploitation patterns. The ability to reliably trace stone tools to their geological sources would provide valuable insights into mobility patterns, territorial ranges, and social interactions in Neolithic societies. Recent studies in the Iberian Peninsula have demonstrated how reliable provenance data can illuminate patterns of prehistoric exchange and social interaction (Bernabeu et al., 2012; Domínguez-Bella & Herrero, 2012).

In conclusion, this proof-of-concept study demonstrates that MoS can provide reliable, distinctive signatures for dolerite sources based on their iron phase compositions. The multiple levels of discrimination possible - from broad magnetic content differences to specific phase combinations and unique markers - offer significant potential for archaeological provenance studies. While additional research is needed to fully develop this approach, the results presented here provide a promising foundation for a new tool in ophitic artifact provenance determination that could enhance our understanding of prehistoric stone tool production and distribution networks.

CRediT authorship contribution statement

J. Jiménez-Puerto: Writing – review & editing, Writing – original draft, Visualization, Validation, Software, Methodology, Investigation, Formal analysis, Data curation, Conceptualization. **E. Devlin:** Writing – review & editing, Writing – original draft, Validation, Methodology, Investigation, Formal analysis, Conceptualization. **G. Gallello:** Writing – review & editing, Resources, Methodology, Investigation, Data curation. **T. Orozco-Köhler:** Resources. **J. Bernabeu Aubán:** Resources, Project administration, Funding acquisition.

Declaration of competing interest

The authors declare that they have no known competing financial interests or personal relationships that could have appeared to influence the work reported in this paper.

Acknowledgments

The authors acknowledge the Ministry of Education, Culture and Sport of the Valencian Government for funding the projects NeoNetS "A Social Network Approach to Understanding the Evolutionary Dynamics of Neolithic Societies (C. 7600-4000 cal. BP)" (Prometeo/2021/007) and The project PROMETEO (CIPROM 2021/036).

Gianni Gallello acknowledges the financial support of the project founded by the Spanish Ministry of Science and Innovation EvolMED "Evolutionary cultural patterns in the contexts of the neolithisation process in the Western Mediterranean" (PID2021-127731NB-C21).

Appendix A. Supplementary data

Supplementary data to this article can be found online at https://doi.org/10.1016/j.jasrep.2025.105289.

Data availability

File with all Supplementary Material

References

Aldenderfer, M., Drennan, R.D., 1998. Statistics for archaeologists: a commonsense approach. J. Field Archaeol. 25 (2), 233. https://doi.org/10.2307/530582.

Ammann, A.A., 2007. Inductively coupled plasma mass spectrometry (ICP MS): a versatile tool. J. Mass Spectrom. 42 (4), 419–427. https://doi.org/10.1002/jms.1206.

Armero, C., García-Donato, G., Jiménez-Puerto, J., Pardo-Gordó, S., & Bernabeu, J. (2020). *Bayesian classification for dating archaeological sites via projectile points*. https://doi.org/10.48550/ARXIV.2012.00657.

Bernabeu Aubán, J., Orozco Köhler, T., Diez Castillo, A., 2002. El poblamiento neolítico: Desarrollo del paisaje agrario en les valls de l'Alcoi. In: *La Sarga. Arte Rupestre y Territorio:[catálogo De La Exposición]*, pp. 171–184.

Bernabeu, J., Molina Balaguer, Ll., Diez Castillo, A., & Orozco Köhler, T. (2006). Inequalities and Power. Three millennia of Prehistory in Mediterranean Spain (5600 – 2000 cal BC). In P. Diaz-del-Rio & L. García (Eds.), *Social Inequality in Iberian Late Prehistory* (pp. 97–116). http://hdl.handle.net/10261/9740.

Bernabeu, J., Moreno, A., Barton, C.M., 2012. In: Complex Systems, Social Networks, and the Evolution Os Social Complexity in the East of Spain from the Neolithic to Pre-Roman times. Routledge, pp. 53–73.

Carrión, F., Gómez, M.T., 1983. Análisis petroarqueológico de los artefactos de piedra trabajada durante la prehistoria reciente en la provincia de Granada. Cuadernos De Prehistoria y Arqueología De La Universidad De Granada 8, 447–477.

Clarke, A.J.I., Kirkland, C.L., Bevins, R.E., Pearce, N.J.G., Glorie, S., Ixer, R.A., 2024. A Scottish provenance for the Altar Stone of Stonehenge. Nature 632 (8025), 570–575. https://doi.org/10.1038/s41586-024-07652-1.

Cornell, R. M., & Schwertmann, U. (2003). The iron oxides: Structure, properties, reactions, occurrences, and uses (Vol. 664). Wiley-vch Weinheim.

Dillmann, P., Balasubramaniam, R., Beranger, G., 2002. Characterization of protective rust on ancient Indian iron using microprobe analyses. Corros. Sci. 44 (10), 2231–2242. https://doi.org/10.1016/S0010-938X(02)00028-8.

Domínguez-Bella, S., Herrero, J.M., 2012. Archaeomineralogy of prehistoric artifacts and gemstones. The Contribution of Mineralogy. International Seminar, Archaeometry and Cultural Heritage, pp. 5–28.

Douvalis, A.P., Polymeros, A., Bakas, T., 2010. IMSG09: a 57 Fe-119Sn Mössbauer spectra computer fitting program with novel interactive user interface. J. Phys. Conf. Ser. 217, 012014. https://doi.org/10.1088/1742-6596/217/1/012014.

Dyar, M.D., Agresti, D.G., Schaefer, M.W., Grant, C.A., Sklute, E.C., 2006. Mössbauer spectroscopy of earth and planetary materials. Annu. Rev. Earth Planet. Sci. 34 (1), 83–125. https://doi.org/10.1146/annurev.earth.34.031405.125049.

Frahm, E., Doonan, R.C.P., 2013. The technological versus methodological revolution of portable XRF in archaeology. J. Archaeol. Sci. 40 (2), 1425–1434. https://doi.org/10.1016/j.jas.2012.10.013.

Froment, F., Tournié, A., Colomban, P., 2008. Raman identification of natural red to yellow pigments: Ochre and iron-containing ores. J. Raman Spectrosc. 39 (5), 560–568. https://doi.org/10.1002/jrs.1858.

Gallello, G., Orozco, T., Pastor, A., De La Guardia, M., Bernabeu, J., 2016. Regional provenance of dolerite prehistoric objects through mineral analysis. Microchem. J. 124, 167–174. https://doi.org/10.1016/j.microc.2015.08.018.

Gangas, N.H.J., Kostikas, A., Simopoulos, A., Vocotopoulou, J., 1971. Mössbauer spectroscopy of ancient greek pottery. Nature 229 (5285), 485–486. https://doi.org/10.1038/229485a0.

Garrido-Pena, R., 1996. Redes de intercambio entre el Sureste y el País Valenciano durante el Calcolítico: Reflexiones en torno a un patrón decorativo campaniforme. Complutum 7, 63–72.

Higgins, M. D. (2006). Quantitative Textural Measurements in Igneous and Metamorphic Petrology (1st ed.). Cambridge University Press. https://doi.org/10.1017/CBO9780511535574.

Hunter, J.D., 2007. Matplotlib: a 2D graphics environment. Comput. Sci. Eng. 9 (03), 90–95.

Jiménez-Puerto, J. (2022). *Conectando con el pasado. Redes sociales en la Prehistoria reciente.* (Proquest). Universidad de Valencia. https://www.proquest.com/docview/2742640164.

Jiménez-Puerto, J., Gallello, G., Orozco, T., 2024. Neural networks to map archaeological lithic artefacts. Inżynieria Mineralna 1 (1). https://doi.org/10.29227/IM-2024-01-41.

Klingelhöfer, G., Morris, R.V., Bernhardt, B., Schröder, C., Rodionov, D.S., De Souza, P. A., Yen, A., Gellert, R., Evlanov, E.N., Zubkov, B., Foh, J., Bonnes, U., Kankeleit, E., Gütlich, P., Ming, D.W., Renz, F., Wdowiak, T., Squyres, S.W., Arvidson, R.E., 2004. Jarosite and hematite at meridiani planum from opportunity's Mössbauer spectrometer. Science 306 (5702), 1740–1745. https://doi.org/10.1126/science.1104653.

Kohonen, T., 1982. Self-organized formation of topologically correct feature maps. Biol. Cybern. 43 (1), 59–69. https://doi.org/10.1007/BF00337288.

Kostikas, A., Simopoulos, A., Gangas, N.H., 1974. Mössbauer studies of ancient pottery. Le Journal De Physique Colloques 35 (C1), C1-107–C. https://doi.org/10.1051/jphyscol:1974133.

Le Maitre, R. W., Streckeisen, A., Zanettin, B., Le Bas, M., Bonin, B., & Bateman, P. (2005). Igneous rocks: A classification and glossary of terms: Recommendations of the International Union of Geological Sciences Subcommission on the Systematics of Igneous Rocks. Cambridge University Press.

Liu, Y., Hu, Z., Gao, S., Günther, D., Xu, J., Gao, C., Chen, H., 2008. In situ analysis of major and trace elements of anhydrous minerals by LA-ICP-MS without applying an internal standard. Chem. Geol. 257 (1–2), 34–43. https://doi.org/10.1016/j.chemgeo.2008.08.004.

Lyubutin, I., Lin, C., Korzhetskiy, Y.V., Dmitrieva, T., Chiang, R., 2009. Mössbauer spectroscopy and magnetic properties of hematite/magnetite nanocomposites. J. Appl. Phys. 106 (3).

McKinney, W., 2010. Data structures for statistical computing in python. Proceedings of the Python in Science Conference 445, 56.

Molera, J., Vendrell-Saz, M., García-Vallés, M., Pradell, T., 1997. Technology and colour development of Hispano-Moresque Lead-Glazed pottery. Archaeometry 39 (1), 23–39. https://doi.org/10.1111/j.1475-4754.1997.tb00788.x.

Molina, L., & Orozco, T. (2011). Producción, consumo e intercambio en el registro material de la Vital. *La Vital (Gandia, Valencia): Vida y Muerte En La Desembocadura Del Serpis Durante El III y El I Milenio aC*, 255–264.

Murad, E., 1998. Clays and clay minerals: what can Mössbauer spectroscopy do to help understand them? Hyperfine Interact. 117 (1), 39–70.

Murad, E., Cashion, J., 2004. Mössbauer spectroscopy of environmental materials and their industrial utilization. Springer, US. https://doi.org/10.1007/978-1-4419-9040-2.

Ogburn, D., Sillar, B., Sierra, J.C., 2013. Evaluating effects of chemical weathering and surface contamination on the in situ provenance analysis of building stones in the Cuzco region of Peru with portable XRF. J. Archaeol. Sci. 40 (4), 1823–1837. https://doi.org/10.1016/j.jas.2012.09.023.

Orozco Köhler, T., & Gallello, G. (2017). *Testing a new methodological approach to define the use of dolerite outcrops for prehistoric tool production in Mediterranean Iberia.*

Orozco-Köhler, T. (1990). El utillaje pulimentado y el instrumental de molienda. *El III Milenio AC En El País Valenciano: Los Poblados de Jovades (Cocentaina, Alacant) y Arenal de La Costa (Ontinyent, València)*, 99–108.

Orozco-Köhler, T. (2000). Aprovisionamiento e Intercambio: Análisis petrológico del utillaje pulimentado en la Prehistoria Reciente del País Valenciano (España) (Vol. 867). British Archaeological Reports Limited.

Papamarinopoulos, S., Readman, P.W., Maniatis, Y., Simopoulos, A., 1987. Palaeomagnetic and mineral magnetic studies of sediments from Petralona cave. Greece. Archaeometry 29 (1), 50–59. https://doi.org/10.1111/j.1475-4754.1987.tb00397.x.

Pedregosa, F., Varoquaux, G., Gramfort, A., Michel, V., Thirion, B., Grisel, O., Blondel, M., Prettenhofer, P., Weiss, R., Dubourg, V., et al., 2011. Scikit-learn: machine learning in Python. The Journal of Machine Learning Research 12, 2825–2830.

Polikreti, K., Murphy, J.M.A., Kantarelou, V., Karydas, A.G., 2011. XRF analysis of glass beads from the Mycenaean palace of Nestor at Pylos, Peloponnesus, Greece: New insight into the LBA glass trade. J. Archaeol. Sci. 38 (11), 2889–2896. https://doi.org/10.1016/j.jas.2011.05.003.

Potts, P.J., Bernardini, F., Jones, M.C., Williams-Thorpe, O., Webb, P.C., 2006. Effects of weathering onin situ portable X-ray fluorescence analyses of geological outcrops: Dolerite and rhyolite outcrops from the Preseli Mountains. South Wales. X-Ray Spectrometry 35 (1), 8–18. https://doi.org/10.1002/xrs.881.

Potts, P.J., West, M. (Eds.), 2008. *Portable X-Ray Fluorescence Spectrometry: Capabilities for in Situ Analysis*. Royal Society of Chemistry. https://doi.org/10.1039/9781847558640.

Přichystal, A. (2013). *Lithic raw materials in prehistoric times of eastern Central Europe*. Masarykova univerzita.

Ramacciotti, M., Gallello, G., Jiménez-Puerto, J., Bernabeu, J., Orozco Köhler, T., Rubio-Barberá, S., Pastor, A., 2022. Non-destructive characterisation of dolerite archaeological artefacts. Microchem. J. 183, 108080. https://doi.org/10.1016/j.microc.2022.108080.

Ricq-de Bouard, M., 1996. with Centre de recherches archéologiques. Pétrographie et sociétés néolithiques en France méditerranéenne, L'outillage en pierre polie. CNRS Éd.

Schaaf, P. (2005). Mössbauer Spectroscopy. In *Encyclopedia of Condensed Matter Physics* (pp. 20–31). Elsevier. https://doi.org/10.1016/B0-12-369401-9/01152-9.

Schwedt, A., Mommsen, H., Zacharias, N., 2004. Post-depositional elemental alterations in pottery: Neutron activation analyses of surface and core samples. Archaeometry 46 (1), 85–101.

Smith, G.D., Clark, R.J.H., 2004. Raman microscopy in archaeological science. J. Archaeol. Sci. 31 (8), 1137–1160. https://doi.org/10.1016/j.jas.2004.02.008.

Stevens, J.G., Zhu, W., 1986. A review of Mössbauer spectroscopic studies of ancient pottery. Hyperfine Interact. 29 (1), 1149–1151.

Sylvester, P.J., Jackson, S.E., 2016. A brief history of laser ablation inductively coupled plasma mass spectrometry (LA–ICP–MS). Elements 12 (5), 307–310. https://doi.org/10.2113/gselements.12.5.307.

Thomas, R. (2013). *Practical Guide to ICP-MS: A Tutorial for Beginners, Third Edition* (0 ed.). CRC Press. https://doi.org/10.1201/b14923.

Van Rossum, G., Drake, F.L., 2014. The python language reference. Wilmington, DE, USA, Python Software Foundation.

Vernon, R. H. (2018). *A Practical Guide to Rock Microstructure* (2nd ed.). Cambridge University Press. https://doi.org/10.1017/9781108654609.

Wagner, F., Kyek, A., 2004. Mössbauer spectroscopy in archaeology: Introduction and experimental considerations. Hyperfine Interact. 154, 5–33.

Wagner, F., Wagner, U., 2004. Mössbauer spectra of clays and ceramics. Hyperfine Interact. 154, 35–82.

Wagner, U., Wagner, F.E., Häusler, W., Shimada, I., 2000. In: The Use of Mössbauer Spectroscopy in Studies of Archaeological Ceramics. Elsevier, pp. 417–443. https://doi.org/10.1016/B978-044450487-6/50064-X.

Waskom, M.L., 2021. Seaborn: Statistical data visualization. Journal of Open Source Software 6 (60), 3021.

Williams-Thorpe, O., Potts, P.J., Webb, P.C., 1999. Field-portable non-destructive analysis of lithic archaeological samples by X-Ray fluorescence instrumentation using a mercury iodide detector: comparison with wavelength-dispersive XRF and a case study in british stone axe provenancing. J. Archaeol. Sci. 26 (2), 215–237. https://doi.org/10.1006/jasc.1998.0323.